Co-ordination Chemistry of Higher Oxidation States. Part 35.[1] Synthetic, Spectroscopic, and Electrochemical Studies of some *mer*- and *fac*-$[OsL_3X_3]/[OsL_3X_3]^+$ Systems ($L = PR_3, AsR_3, SbR_3$, or pyridine; $X = Cl$ or Br): Crystal Structure of *fac*-$[Os(PEt_2Ph)_3Cl_3]\cdot CH_2Cl_2$†

Robert A. Cipriano, William Levason,* Roy A. S. Mould, Derek Pletcher, and Michael Webster
Department of Chemistry, The University, Southampton SO9 5NH

The complexes *mer*-$[OsL_3X_3]$ ($L = PMe_3, PEt_3, PEt_2Ph, PEtPh_2$, or $AsEt_3$; X = Cl or Br) are oxidised by HNO_3–HBF_4 to *mer*-$[OsL_3X_3]BF_4$; *fac*- and *mer*-$[Os(py)_3X_3]BF_4$ (py = pyridine) were obtained similarly, but attempts to oxidise *fac*-$[OsL'_3Cl_3]$ ($L' = PR_3$ or AsR_3) or *mer*-$[Os(SbPh_3)_3X_3]$ to Os^{IV} failed. The osmium(IV) complexes were characterised by i.r., u.v.–visible, ^{31}P n.m.r. spectroscopies, magnetic and conductance measurements, and their properties compared with those of the osmium(III) analogues. Cyclic voltammetry showed that most *mer*-$[OsL_3X_3]^{0/+}$ and the *fac*-$[Os(py)_3X_3]^{0/+}$ couples are electrochemically reversible, but *fac*-$[OsL'_3Cl_3]$ exhibited only completely irreversible oxidation waves at highly positive potentials. The *X*-ray structure of *fac*-$[Os(PEt_2Ph)_3Cl_3]\cdot CH_2Cl_2$ has been determined: space group $P\bar{1}$ with $a = 18.606(2)$, $b = 10.088(2)$, $c = 10.011(4)$ Å, $\alpha = 107.91(3)$, $\beta = 97.23(3)$, $\gamma = 94.85(1)°$, and $Z = 2$; Os–Cl 2.442(3)—2.449(2), Os–P 2.375(2)—2.380(3) Å.

The ease of oxidation of substituted halogeno-complexes of the platinum metals $[ML_nX_{6-n}]^{x-}$ varies in a relatively systematic manner with the nature and number of neutral ligands (L), the halides (X), and with the stereochemistry at the metal centre. For example, oxidation of iridium(III) complexes to iridium(IV) becomes harder in the order $[IrLCl_5]^- <$ *trans*-$[IrL_2Cl_4] <$ *cis*-$[IrL_2Cl_4]$, whilst all attempts to oxidise *mer*- or *fac*-$[IrL_3Cl_3]$ have failed.[2–4] The *trans*-$[OsL_2X_4]^{0/-}$ systems have been thoroughly studied[5,6] but in contrast to the iridium systems there are reports[7–9] that some *mer*-$[OsL_3X_3]$ undergo reversible electrochemical oxidation, although the products have been isolated only for $L = NH_3$.[10] Here we report a systematic study of the oxidation of *mer*- and *fac*-$[OsL_3X_3]$ osmium(III) complexes, and characterisation of the osmium(IV) products.

Results and Discussion

mer-$[OsL_3X_3]$.—The familiar *mer* isomers (where $L = PR_3$, AsR_3, or SbR_3; X = Cl or Br) were obtained by heating OsO_4 in HX–EtOH solution with excess of L,[7,11–13] the reduction proceeding stepwise *via trans*-$[OsO_2L_2X_2]$[7,14] and *trans*-$[OsL_2X_4]$.[6,7,11] The examples used in the present study are listed in Table 1, along with selected spectroscopic data. The phosphine and arsine chloro-complexes are red or orange, the bromides dark purple, whilst *mer*-$[Os(SbPh_3)_3Cl_3]$ is green and the bromide grey. All are air-stable paramagnetic solids (μ = 1.8—2.1 B.M.), very soluble in organic solvents. The spectroscopic data are in good agreement with those in the literature,[11,12,15] and it is notable that often only two ν(OsX) vibrations are observed in the i.r. spectra compared with the three expected [theory (C_{2v}): $2A_1 + B_1$]. Single-crystal *X*-ray structures for *mer*-$[Os(PMe_2Ph)_3Cl_3]$[16] and *mer*-$[Os(SbPh_3)_3Br_3]$[17] are available. The complexes *mer*-$[Os(py)_3X_3]$ (py = pyridine) were made as described[18] from *mer*-$[Os(py)_3I_3]$ and the appropriate halogen. The single-crystal *X*-ray structure of the chloride complex, made by an electrochemical route, has been obtained.[19] Group 16 complexes *mer*-$[OsL'_3X_3]$ ($L' = SR_2$, SeR_2, or TeR_2) appear to be unknown, but the *mer*-$[OsS_3X_3]$ and -$[OsSe_3X_3]$ examples are available in the complexes of the multidentate ligands $S(CH_2CH_2CH_2SMe)_2$[20] and $Se(CH_2CH_2CH_2SeMe)_2$.[21]

fac-$[OsL_3X_3]$.—Facial isomers are much rarer[11,12] and little studied. Three examples (X = Cl; $L = PMe_2Ph$, PEt_2Ph, or $AsMe_2Ph$) were made by the literature route[12] which involves reduction of the *mer* isomer with $NaBH_4$ to form $[OsH_4L_3]$, and reaction of this with HCl in methanol. The protonation of $[OsH_4L_3]$ appears to be very dependent upon the particular L,[22] and attempts to synthesise *fac* isomers with a number of other ligands either failed or gave extremely low yields. Shaw and co-workers[23] showed that facile *mer* ⟶ *fac* isomerisation of $[IrL_3Cl_3]$ occurred upon irradiation of the *mer* isomer in benzene with fluorescent light. However we found that *mer*-$[Os(PMe_2Ph)_3Cl_3]$ in benzene was recovered unchanged after 96 h of irradiation. Refluxing $[OsX_6]^{2-}$ (X = Cl or Br) with pyridine (py) in dimethylformamide gave red-brown $[Os(py)_3X_3]$.[24,25] The spectroscopic data (Table 1) are quite different from those of the *mer* isomers,[18] and hence their identity as *fac* forms are confirmed.

Structure of fac-$[Os(PEt_2Ph)_3Cl_3]\cdot CH_2Cl_2$.—The structure of a discrete molecule is shown in Figure 1, and Table 2 lists selected bond lengths and angles. The ligands are arranged in the *fac* geometry whereas all previous reported[26] octahedral osmium(III) complexes characterised by *X*-ray diffraction report the *mer* isomer. The Cl–Os–Cl angles are <90° [85°(av.)] and the P–Os–P angles >90° [103°(av.)]. The molecule has an approximate C_3 axis (Figure 1) with respect to the OsP_3Cl_3 residue which extends to the orientation of the phenyl groups, but to a lesser extent to the methyl groups. The Os–Cl distances [2.446 Å(av.)] are very similar to the Os–Cl(*trans* P) distance in *mer*-$[Os(PMe_2Ph)_3Cl_3]$[16] [2.439(6) Å], but the Os–P

---

† *fac*-Trichlorotris(diethylphenylphosphine)osmium(III)–methylene dichloride (1/1).

Supplementary data available: see Instructions for Authors, *J. Chem. Soc., Dalton Trans.*, 1990, Issue 1, pp. xix—xxii.

Non-S.I. unit employed: B.M. ≈ 0.927×10^{-23} A m^2.

Table 1. Selected spectroscopic data for osmium(III) compounds

Compound	$\nu(OsX)^a$/cm^{-1}	$E_{max.}/10^3$ cm^{-1} (ε_{mol}/dm^3 mol^{-1} cm^{-1})^b		
		$\sigma_L \longrightarrow t_{2g}(Os)$	$\sigma_L + \sigma_X \longrightarrow t_{2g}(Os)$	$\pi_X \longrightarrow t_{2g}(Os)$
mer isomers				
$[Os(PMe_3)_3Cl_3]$	306, 260	20.3 (900)	25.0 (2 460)	26.3 (sh), 30.3 (1 090), 33.6 (2 440)
$[Os(PEt_3)_3Cl_3]$	301, 254	19.4 (890)	24.3 (2 110)	26.5 (1 195), 30.1 (1 120), 33.1 (2 225)
$[Os(PMe_2Ph)_3Cl_3]$	308, 266	19.3 (640)	23.4 (1 470)	27.1 (sh), 30.2 (sh)
$[Os(PEt_2Ph)_3Cl_3]$	300, 255	18.6 (730)	23.1 (1 505)	26.3 (910), 29.6 (1 695), 33.8 (2 670)
$[Os(PEtPh_2)_3Cl_3]$	306, 250	18.8 (760)	22.8 (1 430)	27.5 (2 080), 31.1 (sh)
$[Os(AsEt_3)_3Cl_3]$	305, 270	19.8 (895)	24.3 (1 205)	27.3 (480), 31.6 (1 110), 33.6 (1 490)
$[Os(AsMe_2Ph)_3Cl_3]$	274	20.25 (880)	24.15 (2 070)	27.25 (1 150), 31.9 (sh), 33.9 (sh)
$[Os(SbPh_3)_3Cl_3]$	317, 302	17.1 (655)	21.3 (1 775)	25.7 (1 775), 28.4 (2 430), 34.8 (29 440)
$[Os\{S[(CH_2)_3SMe]_2\}Cl_3]^c$	310, 298 (sh), 284	[19.3 (39), 23.0 (220) (sh)]^d		26.2 (955) (sh), 29.2 (2 450)
$[Os(PMe_3)_3Br_3]$	225 (sh), 200	18.4 (3 300)	21.9 (2 300)	25.3 (1 800), 29.4 (1 700)
$[Os(PEt_3)_3Br_3]$	222, 192	17.4 (2 025)	20.0 (1 435)	22.3 (1 420), 25.0 (1 390), 29.6 (1 495)
$[Os(PEtPh_2)_3Br_3]$	219, 208	17.9 (460)	21.1 (580)	24.0 (sh), 29.4 (2 500)
$[Os(AsEt_3)_3Br_3]$	221, 211 (sh), 198	17.3 (1 990)	20.6 (1 870)	22.6 (1 300), 25.9 (1 390), 30.0 (1 770)
$[Os(SbPh_3)_3Br_3]$	n.o.	15.3 (750)	18.3 (1 100)	20.75 (590), 24.9 (sh), 26.8 (1 310)
$[Os\{S[(CH_2)_3SMe]_2\}Br_3]^c$	223 (sh), 207	[20.1 (1 208) (sh)]^d		22.7 (6 870), 25.9 (1 730) (sh)
fac isomers				
$[Os(PMe_2Ph)_3Cl_3]$	293, 256	19.5 (240), 19.9 (sh)		27.3 (sh), 31.65 (sh), 32.7 (1 910)
$[Os(PEt_2Ph)_3Cl_3]$	292, 252	18.4 (sh) (180), 18.7 (190)		25.2 (sh), 30.3 (710), 31.7 (670)
$[Os(AsMe_2Ph)_3Cl_3]$	258	20.5 (150)		24.3 (sh), 28.8 (1 240), 31.1 (1 060)
$[Os(py)_3Cl_3]$	313, 288			24.3 (sh), 29.4 (sh), 31.75 (5 880)
$[Os(py)_3Br_3]$	196			21.9 (1 080), 25.0 (5 510), 30.95 (11 430)

[a] Nujol mull. [b] In CH_2Cl_2 solution. Weak features between 4 000 and 9 000 cm^{-1} are intraconfigurational bands. [c] Data from ref. 20. [d] Not assigned.

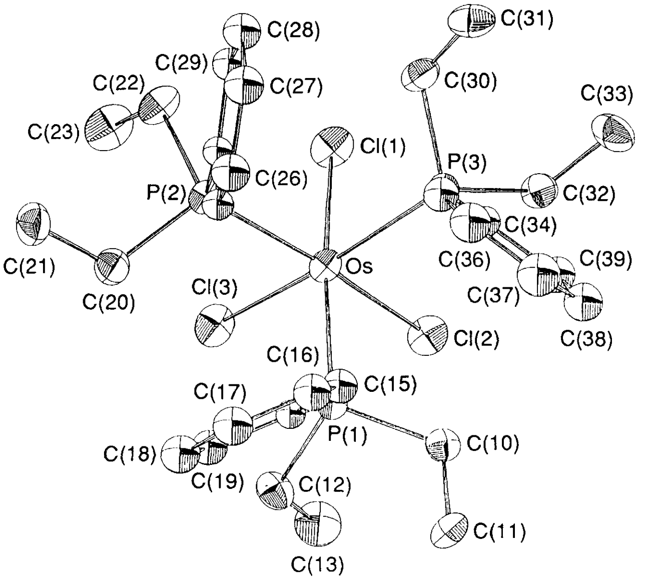

Figure 1. View of the discrete molecule *fac*-$[Os(PEt_2Ph)_3Cl_3]$ showing the atom-numbering scheme. The atom surfaces are drawn at the 40% probability level and H atoms omitted for clarity

distances [2.378 Å(av.)] are rather longer (0.03 Å) than the Os–P(*trans* Cl) in the same compound.

mer-$[OsL_3X_3]BF_4$.—The electrochemical data (below) show that most *mer*-$[OsL_3X_3]$ undergo reversible one-electron oxidations, and a variety of oxidising agents were explored in attempts to achieve this transformation chemically. For L = PR_3 or AsR_3, halogens tend to remove one ligand to form *trans*-$[OsL_2X_4]$.[6] No reaction was apparent using $FeCl_3$ in EtOH {*cf.* ref. 10 where $FeCl_3$ was used to form *mer*-$[Os(NH_3)_3X_3]^+$}, or $KMnO_4$–18-crown-6 (1,4,7,10,13,16-hexaoxacyclo-octadecane) in toluene. The reactions of $AgBF_4$ with *mer*-$[OsL_3X_3]$ in CH_2Cl_2 slowly produced silver mirrors,

Table 2. Selected bond lengths (Å) and angles (°) for *fac*-$[Os(PEt_2Ph)_3Cl_3]\cdot CH_2Cl_2$

Os–Cl(1)	2.442(3)	P(1)–C(10)	1.837(9)
Os–Cl(2)	2.447(2)	P(1)–C(12)	1.840(10)
Os–Cl(3)	2.449(2)	P(1)–C(14)	1.833(9)
Os–P(1)	2.380(3)	P(2)–C(20)	1.830(10)
Os–P(2)	2.380(2)	P(2)–C(22)	1.838(9)
Os–P(3)	2.375(2)	P(2)–C(24)	1.839(9)
		P(3)–C(30)	1.828(10)
Cl • • • Cl (min.)	3.28	P(3)–C(32)	1.829(9)
Cl • • • P (min.)	3.12	P(3)–C(34)	1.822(9)
P • • • P (min.)	3.68		
C–C (ethyl)	max. 1.54(1)	min. 1.51(1)	mean 1.52(1)
C–C (phenyl)	max. 1.42(1)	min. 1.33(1)	mean 1.38(2)
Cl(1)–Os–Cl(2)	84.4(1)	P(1)–C(10)–C(11)	115.4(7)
Cl(1)–Os–Cl(3)	85.8(1)	P(1)–C(12)–C(13)	116.0(7)
Cl(2)–Os–Cl(3)	84.5(1)	P(1)–C(14)–C(15)	119.5(7)
P(1)–Os–P(2)	103.9(1)	P(1)–C(14)–C(19)	122.6(7)
P(1)–Os–P(3)	104.6(1)	P(2)–C(20)–C(21)	116.5(7)
P(2)–Os–P(3)	101.5(1)	P(2)–C(22)–C(23)	115.1(7)
P(1)–Os–Cl(2)	81.7(1)	P(2)–C(24)–C(25)	120.0(7)
P(1)–Os–Cl(3)	87.3(1)	P(2)–C(24)–C(29)	120.9(7)
P(2)–Os–Cl(1)	88.6(1)	P(3)–C(30)–C(31)	121.0(7)
P(2)–Os–Cl(3)	83.6(1)	P(3)–C(32)–C(33)	116.7(7)
P(3)–Os–Cl(1)	80.6(1)	P(3)–C(34)–C(35)	119.3(7)
P(3)–Os–Cl(2)	88.6(1)	P(3)–C(34)–C(39)	121.2(7)
Os–P(1)–C(10)	113.9(3)	Os–P(2)–C(24)	119.2(3)
Os–P(1)–C(12)	116.7(4)	Os–P(3)–C(30)	112.8(3)
Os–P(1)–C(14)	119.0(3)	Os–P(3)–C(34)	118.6(3)
Os–P(2)–C(20)	114.6(3)	Os–P(3)–C(32)	112.6(3)
Os–P(2)–C(22)	116.1(3)		
C–P–C	max. 104.0(5)	min. 100.3(4)	
C–C–C	max. 122.2(9)	min. 117.8(9)	

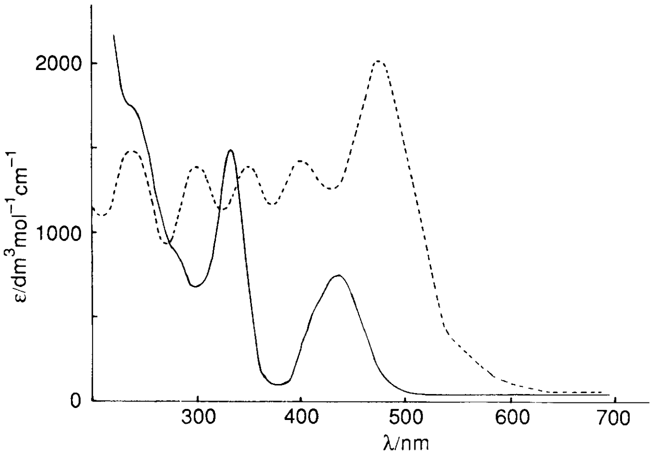

Figure 2. U.v.–visible spectra of *mer*-[$Os(PEt_2Ph)_3Cl_3$] (——) and *mer*-[$Os(PEt_3)_3Br_3$] (– – –) in CH_2Cl_2

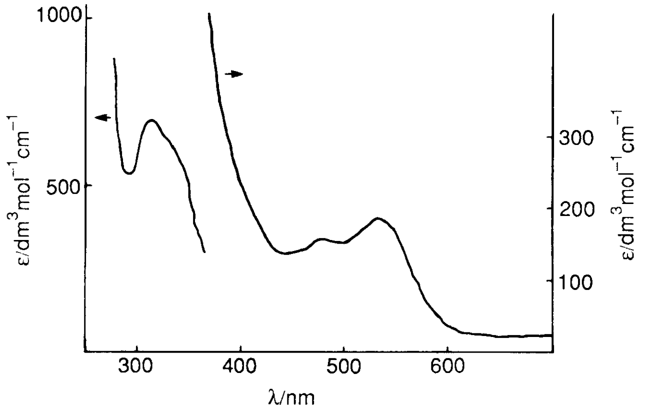

Figure 3. U.v.-visible spectrum of *fac*-[$Os(PEt_2Ph)_3Cl_3$] in CH_2Cl_2

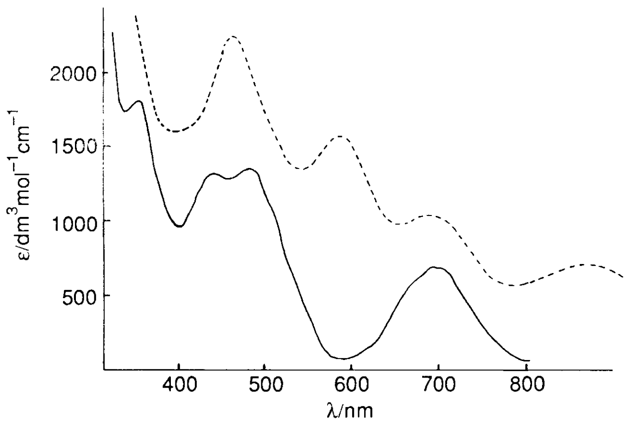

Figure 4. U.v.–visible spectra of *mer*-[$Os(PMe_3)_3Cl_3]^+$ (——) and *mer*-[$Os(PEt_2Ph)_3Br_3]^+$ (– – –) in CH_2Cl_2

but the expected [$OsL_3X_3]BF_4$ could not be isolated from the filtrates; the subsequently established instability of the products in solution probably accounts for the failure of this route. The complexes *mer*-[$OsL_3X_3]BF_4$ were finally obtained by treatment of the appropriate [OsL_3X_3] suspended in 40% aqueous HBF_4 at 0 °C with concentrated HNO_3. The reaction rate varies with complex, probably reflecting the low solubilities in the aqueous acid, and completion of the oxidation was established by removing samples of the product from time to time and examining the u.v.–visible spectra. Although oxidation was apparent on the cyclic voltammetry time-scale (below), all attempts chemically to oxidise *mer*-[$Os(SbPh_3)_3X_3$] caused decomposition. The complex *mer*-[$Os(py)_3Cl_3$]Cl was most readily prepared by treatment of *mer*-[$Os(py)_3I_3$] [18] with excess of chlorine in CH_2Cl_2, whilst the bromide analogue was made by the usual HNO_3–HBF_4 route from the osmium(III) complex.

The complex *mer*-[$Os\{S(CH_2CH_2CH_2SMe)_2\}Br_3]BF_4$ was made from concentrated HNO_3–HBF_4 and the osmium(III) analogue, but attempts to isolate samples of the chloro-complex, or of the corresponding triselenoether complexes, failed. Oxidation of the osmium(III) complexes occurred readily as evidenced by *in situ* u.v.–visible studies, but the products were soluble in the acid media from which they could not be recovered in a pure state. The formation of a *mer*-[$OsS_3X_3]^+$ species by this route contrasts with the direct reaction of [$OsX_6]^{2-}$ with the trithioether which gave *cis*-[$Os\{S(CH_2CH_2CH_2SMe)_2\}X_4$] ($OsS_2X_4$).[20]

The *mer*-[$OsL_3X_3]BF_4$ complexes are red or purple paramagnetic solids (μ *ca.* 1.6 B.M.), stable for some months in the solid state. Comparison of the far-i.r. spectra of corresponding [$OsL_3X_3]^{0/+}$ show that the ν(OsX) vibrations occur *ca.* 20—30 cm^{-1} higher in frequency for the osmium(IV) complexes. The complexes dissolve easily in chlorocarbons and in MeCN, and freshly prepared *ca.* 10^{-3} mol dm^{-3} solutions in MeCN are 1:1 electrolytes (Table 3). The *trans*-[OsL_2X_4] complexes, despite their paramagnetism, exhibited ^{31}P-$\{^1H\}$ n.m.r. spectra although the resonances were very greatly shifted to low frequency from the free-ligand values (*ca.* –1 200 p.p.m. from H_3PO_4).[6,27] Hence the ^{31}P-$\{^1H\}$ n.m.r. spectra of *mer*-[$Os(PEt_3)_3X_3]^+$ were examined over the range +400 to –1 500 p.p.m. In freshly prepared CH_2Cl_2 solution, two resonances in the intensity ratio 1:2 were observed (Table 4) in the region –20 to –40 p.p.m. Under high resolution the resonances appeared as a triplet and doublet respectively consistent with a *mer* geometry. When the solutions were allowed to stand these resonances decreased in intensity and new features corresponding to free PEt_3, $OPEt_3$, and *trans*-[$Os(PEt_3)_2X_4$] appeared.[6] No resonances were seen for *mer*-[$Os(PR_3)_3X_3$], but it is notable that *mer*-[$Re(PMe_2Ph)_3Cl_3$], which is isoelectronic with the osmium(IV) complexes, exhibits ^{31}P-$\{^1H\}$ signals at +38.6 and –24.0 p.p.m.[28] The spectra of *mer*-[$Os(PMe_3)_3X_3]^+$ show single very broad resonances with ill defined structure which we assume result from near coincidence of the resonances of the inequivalent phosphines. Again these resonances disappear on standing being replaced by those of $OPMe_3$ and *trans*-[$Os(PMe_3)_2X_4$]. The mass balance for the decomposition of *mer*-[$OsL_3X_3]^+$ requires other osmium species to be formed in addition to the *trans* isomers, but these were not evident in the n.m.r. spectra, and are presumably n.m.r.-silent osmium(III) materials. This decomposition in solution is also evident in the u.v.–visible spectra, which over a period of time develop absorptions characteristic of the *trans*-[OsL_2X_4] complexes;[6] however the complexity of the spectra of these decomposed solutions is too great for other species present to be identified. The solution instability has also precluded attempts to grow crystals for an *X*-ray study of one of these cations.

fac-[$Os(py)_3X_3]BF_4$.—These two complexes were readily isolated by HNO_3–HBF_4 treatment of the osmium(III) analogues, but attempts to prepare facial osmium(IV) complexes with phosphine ligands were unsuccessful, correlating with the completely irreversible oxidations observed electrochemically.

U.V.–Visible Spectra.—The complexes of Os^{III} and Os^{IV} have rich u.v.–visible spectra (Tables 1 and 3) and typical examples are shown in Figures 2—4. The assignments below are based upon previous studies of the osmium(III) complexes,[29–31] and

Table 3. Physical and spectroscopic data for $[OsL_3X_3]BF_4$

Compound	Colour	$\nu(OsX)^a/cm^{-1}$	$E_{max.}/10^3\ cm^{-1}\ (\varepsilon_{mol}/dm^3\ mol^{-1}\ cm^{-1})^b$			$\Lambda_M{}^c/\Omega^{-1}\ cm^2\ mol^{-1}$
			$\sigma_L \longrightarrow t_{2g}(Os)$	$\sigma_L + \sigma_X \longrightarrow t_{2g}(Os)$	$\pi_X \longrightarrow t_{2g}(Os)$	
mer						
$[Os(PMe_3)_3Cl_3]BF_4$	Dark red	338, 282	14.6 (690)	19.95 (sh), 20.35 (1 370)	21.9 (1 340), 26.95 (1 800), 31.45 (3 940)	—
$[Os(PEt_3)_3Cl_3]BF_4$	Dark red	331, 281	13.4 (830)	19.4 (1 650)	22.4 (1 450), 31.55 (4 880)	141
$[Os(PEt_2Ph)_3Cl_3]BF_4$	Brown	334, 280	12.35 (420)	19.25 (sh)	21.3 (sh), 23.2 (1 410), 26.4 (1 600), 31.45 (sh)	—
$[Os(PEtPh_2)_3Cl_3]BF_4$	Brown	342, 300 (sh), 291	12.5[d]	19.5 (sh)	23.8, 29.1	96
$[Os(AsEt_3)_3Cl_3]BF_4$	Dark red	328, 285	13.2 (1 000)	19.0 (1 510)	22.8 (1 390), 27.1 (3 710)	133
$[Os(py)_3Cl_3]Cl$	Orange	349, 317	—	—	21.7 (920), 27.9 (3 603)	—
$[Os(PMe_3)_3Br_3]BF_4$	Purple	241, 220	13.75 (1 130)	n.o.	18.2 (3 150), 20.2 (sh), 21.6 (4 040), 27.0 (sh), 29.4 (1 640)	—
$[Os(PEt_3)_3Br_3]BF_4$	Red-purple	227 (br)	12.7 (810)	15.4 (730)	18.2 (1 910), 21.65 (3 420), 27.2 (2 000)	137
$[Os(PEt_2Ph)_3Br_3]BF_4$	Brown-purple	236, 217	11.7 (630)	14.6 (980)	17.0 (1 550), 21.2 (2 270)	149
$[Os(PEtPh_2)_3Br_3]BF_4$	Brown-purple	n.o.	11.8 (sh)[d]	14.4	18.0, 20.5, 24.0 (sh), 28.5	—
$[Os(AsEt_3)_3Br_3]BF_4$	Purple	227, 210 (sh)	12.1 (1 010)	15.4 (1 640)	17.9 (2 250), 22.0 (2 220), 26.9 (3 570)	120
$[Os\{S[(CH_2)_3SMe]_2\}Br_3]BF_4$	Purple	247, 210	15.0 (750)[e]		18.5 (3 930), 19.5 (sh), 22.1 (2 250), 30.5 (1 170)	121
$[Os(py)_3Br_3]BF_4$	Brown	n.o.	—	—	22.3 (1 500), 25.0 (2 600)	—
fac						
$[Os(py)_3Cl_3]BF_4$	Orange-brown	348, 308	—	—	21.6 (≈1 800), 27.7 (≈7 100)[f]	—
$[Os(py)_3Br_3]BF_4$	Purple	248, 217	15.4 (960)[e]		19.3 (3 480), 25.25 (3 020), 26.7 (3 230), 31.1 (5 240)	118

[a] Nujol mull; n.o. = not observed. [b] In CH_2Cl_2 solution. [c] *ca.* 10^{-3} mol dm^{-3} in MeCN; 1 : 1 electrolytes have $\Lambda_M = 120—160\ \Omega^{-1}\ cm^2\ mol^{-1}$. [d] Diffuse reflectance. [e] See text. [f] ε_{mol} only approximate due to solubility problems.

Table 4. ^{31}P-{^{1}H} N.m.r. data for some *mer* osmium(IV) complex cations

Complex	$\delta(^{31}P)$/p.p.m. $(^{2}J_{PP}/Hz)^{a}$		
$[Os(PMe_3)_3Cl_3]^+$	−33.4 (m)[b]		[−1 221][c]
$[Os(PMe_3)_3Br_3]^+$	−23.5 (m)[b]		[−1 285][c]
$[Os(PEt_3)_3Cl_3]^+$	−34.0 (t) (25)	−37.0 (d) (25)	[−1 210][c]
$[Os(PEt_3)_3Br_3]^+$	−26.6 (t) (25)	−32.0 (d) (25)	[−1 236][c]
$[Os(PEt_2Ph)_3Br_3]^+$	−29.0 (t) (28)	−36.0 (d) (28)	

[a] In CH_2Cl_2–CD_2Cl_2 solution relative to 85% H_3PO_4. [b] Complex multiplet, see text. [c] Resonance of $[OsL_2X_4]$ decomposition product, see ref. 6.

Table 5. Cyclic voltammetry data [*] for *mer*-$[OsL_3X_3]$ complexes

mer Complex	E_c°/V *vs.* s.c.e. X = Cl	Br
$[Os(PMe_3)_3X_3]$	0.99	1.03
$[Os(PEt_3)_3X_3]$	0.91	0.92
$[Os(PMe_2Ph)_3X_3]$	1.07	
$[Os(PEt_2Ph)_3X_3]$	1.01	
$[Os(PEtPh_2)_3X_3]$	0.99	0.95
$[Os(AsEt_3)_3X_3]$	0.86	0.88
$[Os(SbPh_3)_3X_3]$	1.16 (−0.21)	1.10 (−0.15)
$[Os(py)_3X_3]$	0.98	1.05
$[Os\{S(CH_2CH_2CH_2SMe)_2\}X_3]$	1.17 (−0.27)	1.17 (−0.40)
$[Os\{Se(CH_2CH_2CH_2SeMe)_2\}X_3]$		1.06 (−0.35)

[*] Formal potentials *vs.* the standard calomel electrode (s.c.e.) determined by cyclic voltammetry in CH_2Cl_2 containing 0.1 mol dm^{-3} $NBu^n{}_4BF_4$. The potential of ferrocene under these conditions is 0.58 V. Values in parentheses are for the reversible Os^{III}–Os^{II} couples.

our own study of *trans*-$[OsL_2X_4]^{0/-}$.[6] It is convenient to deal with each type of complex in turn.

mer-$[OsL_3X_3]$. Apart from weak features $<10\,000$ cm^{-1} which are intraconfigurational bands, the spectra are dominated by L, X $\longrightarrow$ Os charge-transfer (c.t.) transitions. In these complexes the low symmetry (C_{2v}) will result in considerable orbital mixing, and assignments of transitions from specific ligand orbitals to t_{2g}(Os)[*] are less realistic than for higher-symmetry complexes. For *mer*-$[OsL_3Cl_3]$ where L = PR_3, AsR_3, or SbR_3, we have distinguished three major regions of absorption (Table 1). The lowest-energy features listed in each spectrum which vary with L are assigned to $\sigma L \longrightarrow t_{2g}(Os)$ c.t. transitions from the mutually *trans* L groups. The next features at some *ca.* 5 000 cm^{-1} higher frequency are from the mixed $\sigma L + \sigma Cl \longrightarrow t_{2g}(Os)$, whilst the strong bands $\geqslant 26\,000$ cm^{-1} are mainly $\pi Cl \longrightarrow t_{2g}(Os)$ c.t. in character. For the corresponding *mer*-$[OsL_3Br_3]$ similar assignments are proposed (Table 1). It should be noted that the '$\sigma L \longrightarrow t_{2g}(Os)$' transitions in the bromides lie 2 000—3 000 cm^{-1} to lower energy than in the chlorides, reinforcing the qualification made above about orbital mixing.

fac-$[OsL_3Cl_3]$ (L = PR_3 *or* AsR_3). The spectra are somewhat simpler than those of the *mer* isomers, as mixing of σ L and σ X will be less important in the higher symmetry.[31] The bands at *ca.* 18 000—21 000 cm^{-1} will have predominantly $\sigma L \longrightarrow t_{2g}(Os)$ character, whilst the features at *ca.* 24 000 cm^{-1} are $\pi Cl \longrightarrow t_{2g}(Os)$. The intense bands assigned as $\sigma L + \sigma X \longrightarrow t_{2g}(Os)$ for the *mer* isomers are absent, and this difference appears to be a convenient method of distinguishing the two isomers, despite the richness of the spectra.

mer-$[OsL_3X_3]^+$. Due to the instability in solution of the osmium(IV) cations, spectra were recorded immediately upon dissolution of the solids in CH_2Cl_2. Even so it proved impossible to obtain reproducible solution spectra from the least-stable *mer*-$[Os(PEtPh_2)_3X_3]^+$, and for these two compounds diffuse-reflectance data obtained from the solids are given in Table 3. For the phosphine and arsine complexes, the assignments follow straightforwardly from those of the osmium(III) analogues, with the major bands shifted to low energy by 3 000—6 000 cm^{-1} for the osmium(IV) compounds, although since the electron-pairing energy corrections are different for d^4 and d^5 ions strict numerical comparison is not justified.[32]

For both *mer*- and *fac*-$[Os(py)_3X_3]^+$ and *mer*-$[Os\{S(CH_2CH_2CH_2SMe)_2\}Br_3]^+$ the major observed features in the spectra are assignable to $\pi X \longrightarrow t_{2g}(Os)$ transitions. The weak feature in the thioether spectrum at 15 000 cm^{-1} may be $\pi S \longrightarrow t_{2g}(Os)$, but the c.t. transitions involving the pyridine groups are not evident. The assignment of the feature at 15 400 cm^{-1} for the *fac* bromo-complex is unclear, since it is not present for the other pyridine complexes.

Electrochemical Studies.—Cyclic voltammetry was used to determine the formal potentials of the Os^{IV}–Os^{III} couples. Voltammograms were recorded at potential scan rates over the range 0.03—0.3 V s^{-1} at a polished, vitreous carbon disc electrode for 10^{-3} mol dm^{-3} solutions of the complexes in CH_2Cl_2–$NBu^n{}_4BF_4$ (0.1 mol dm^{-3}). The data for the *mer*-$[OsL_3X_3]$ complexes are reported in Table 5; all gave voltammograms which confirmed that the Os^{IV}–Os^{III} couples were reversible and hence that all the osmium(IV) species were stable on the time-scale of cyclic voltammetry (*ca.* 30 s). The formal potentials in Table 5 are consistent with the values reported previously for single complexes.[7,9] It can be seen that the formal potentials are only weakly dependent on the choice of either the neutral ligand or the halide and this mirrors the results from earlier studies of similar Os^{IV}–Os^{III} couples.[10] The voltammograms also show peaks for the reduction of the osmium(III) complexes.[8] The chemistry is however, very varied; a few complexes show reversible Os^{III}–Os^{II} couples (see Table 5) but most show one or more irreversible reduction steps and this behaviour was not investigated.

Cyclic voltammograms were also recorded for the *fac*-$[Os(py)_3X_3]$ complexes in the same medium. The complexes both showed reversible Os^{IV}–Os^{III} couples with formal potentials of 0.99 and 1.04 V for X = Cl and Br respectively. All other *fac* complexes studied showed only totally irreversible oxidation peaks at very positive potentials around +1.5 V.

Conclusion

The comparison of the Os^{IV}–Os^{III} potentials for *trans*-$[OsL_2X_4]^6$ and *mer*-$[OsL_3X_3]^+$ reveals that replacement of one X by L shifts the redox potential to more positive values by *ca.* 0.6 V. The complexes *mer*-$[OsL_3X_3]^+$ are stable for L = py, but those of L = PR_3 or AsR_3 decompose quite rapidly in solution. The effect of stereochemistry is evident in the failure of *fac*-$[OsL'_3X_3]$ to show reversible oxidation even upon the short time-scale of cyclic voltammetry, although with the weaker field ligand pyridine isolation of the *fac* isomers is possible.

Experimental

Osmium tetraoxide and sodium hexachloro-osmate(IV) were obtained from Johnson Matthey Chemicals Ltd. and used

---

[*] Although the t_{2g} label refers strictly to O_h symmetry and is incorrect for lower symmetries, it is used here as a convenient shorthand for the lower three osmium *d* orbitals.

Table 6. Atomic co-ordinates with standard deviations in parentheses for *fac*-$[Os(PEt_2Ph)_3Cl_3]\cdot CH_2Cl_2$

Atom	*x*	*y*	*z*	Atom	*x*	*y*	*z*
Os	0.278 28(2)	0.271 64(5)	0.372 29(4)	C(23)	0.082 6(7)	0.050 2(13)	0.384 5(12)
Cl(1)	0.272 6(1)	0.071 5(3)	0.460 9(3)	C(24)	0.166 3(5)	0.097 9(9)	0.025 1(9)
Cl(2)	0.376 6(1)	0.376 3(3)	0.574 4(2)	C(25)	0.170 4(5)	0.188 6(10)	−0.053 3(10)
Cl(3)	0.197 9(1)	0.369 1(3)	0.543 6(3)	C(26)	0.172 8(5)	0.139 0(11)	−0.197 9(11)
P(1)	0.298 4(1)	0.498 8(3)	0.348 2(2)	C(27)	0.171 9(6)	−0.004 2(11)	−0.265 5(12)
P(2)	0.166 2(1)	0.167 5(3)	0.217 7(2)	C(28)	0.166 2(5)	−0.097 0(11)	−0.189 1(11)
P(3)	0.363 6(1)	0.143 6(3)	0.245 7(2)	C(29)	0.163 4(5)	−0.046 0(10)	−0.043 5(10)
C(10)	0.395 2(5)	0.564 1(10)	0.363 0(10)	C(30)	0.328 6(5)	−0.041 9(10)	0.157 2(11)
C(11)	0.410 1(5)	0.706 8(11)	0.343 4(11)	C(31)	0.361 2(6)	−0.131 0(11)	0.031 2(11)
C(12)	0.265 3(5)	0.642 9(11)	0.478 7(10)	C(32)	0.446 5(5)	0.138 5(10)	0.362 4(10)
C(13)	0.308 7(7)	0.692 3(13)	0.629 2(12)	C(33)	0.499 2(6)	0.041 4(12)	0.295 8(12)
C(14)	0.260 5(5)	0.524 3(9)	0.181 1(9)	C(34)	0.397 6(5)	0.200 2(10)	0.106 6(10)
C(15)	0.295 3(5)	0.480 0(10)	0.063 4(10)	C(35)	0.354 5(5)	0.161 7(10)	−0.028 7(10)
C(16)	0.269 2(5)	0.495 8(11)	−0.066 0(11)	C(36)	0.379 2(6)	0.210 3(12)	−0.132 6(12)
C(17)	0.206 7(6)	0.554 5(11)	−0.077 4(12)	C(37)	0.442 2(6)	0.292 8(12)	−0.106 4(13)
C(18)	0.169 8(6)	0.600 3(11)	0.035 5(11)	C(38)	0.486 0(6)	0.332 1(11)	0.022 8(11)
C(19)	0.196 6(5)	0.583 7(10)	0.165 5(11)	C(39)	0.464 3(5)	0.284 3(10)	0.132 8(11)
C(20)	0.096 6(5)	0.285 8(11)	0.222 1(11)	Cl(51)*	0.052 5(2)	0.667 1(5)	0.477 3(5)
C(21)	0.023 3(6)	0.222 5(12)	0.130 6(12)	Cl(52)*	−0.004 5(2)	0.632 0(5)	0.185 7(5)
C(22)	0.118 2(6)	0.015 5(11)	0.248 7(10)	C(50)*	−0.025 3(9)	0.632 4(19)	0.349 2(19)

* Atom of CH_2Cl_2 solvate molecule.

as received. Sodium hexabromo-osmate(IV) was made by repeatedly evaporating $Na_2[OsCl_6]$ to dryness with 47% aqueous HBr. Infrared spectra were obtained from Nujol mulls between CsI plates, on a Perkin-Elmer 983G spectrometer. U.v.–visible spectra were measured on a Perkin-Elmer 554 spectrometer, using 1-cm matched quartz cells, or when necessary the diffuse-reflectance attachment of the instrument with $BaSO_4$ as diluent and reference. Magnetic measurements were made with the Johnson Matthey magnetic susceptibility balance, and conductivity measurements using a Pye conductivity bridge with a cell fitted with platinised 1-cm^2 platinum electrodes. Cyclic voltammograms were run using a model DT2101 Hi-tek Potentiostat connected to a Hi-tek PPR1 waveform generator, and were recorded on a Gould series 60 000 X-Y recorder. The working electrode was a vitreous carbon disc, area 0.07 cm^2, and the reference a Radiometer type K401 saturated calomel electrode. Solutions contained 10^{-3} mol dm^{-3} of complex and 0.1 mol dm^{-3} $NBu^n{}_4BF_4$. Ferrocene was run as a standard. N.m.r. spectra were obtained on a Bruker AM360 spectrometer.

mer-$[OsL_3X_3]$ (L = PMe_3, PEt_2Ph, *or* $PEtPh_2$, X = Cl *or* Br; L = PMe_2Ph *or* $AsMe_2Ph$, X = Cl).—These complexes were made by the method of Chatt *et al.*[11] The ligand (4.2 mmol) was added to a nitrogen-purged solution of OsO_4 (0.3 g, 1.2 mmol) and concentrated HX (2 cm^3) in ethanol (30 cm^3), and the solution refluxed for *ca.* 2 h. In some cases, u.v.–visible spectra of the product solutions revealed incomplete reduction, and here further ligand was added and the reflux continued. The solutions were evaporated under reduced pressure to *ca.* 10 cm^3 and stored at 0 °C overnight. The orange-red (Cl) or brown-purple (Br) product was filtered off, washed with diethyl ether (2 × 10 cm^3), and dried *in vacuo*. Yields typically 55% {Found: C, 20.5; H, 5.0. $[Os(PMe_3)_3Cl_3]$, $C_9H_{27}Cl_3OsP_3$ requires C, 20.6; H, 5.1. Found: C, 16.5; H, 4.2. $[Os(PMe_3)_3Br_3]$, $C_9H_{27}Br_3OsP_3$ requires C, 16.4; H, 4.1. Found: C, 45.0; H, 5.8. $[Os(PEt_2Ph)_3Cl_3]$, $C_{30}H_{45}Cl_3OsP_3$ requires C, 45.3; H, 5.7. Found: C, 40.4; H, 4.5. $[Os(PMe_2Ph)_3Cl_3]$, $C_{24}H_{33}Cl_3OsP_3$ requires C, 40.5; H, 4.6. Found: C, 34.1; H, 4.0. $[Os(AsMe_2Ph)_3Cl_3]$, $C_{24}H_{33}As_3Cl_3Os$ requires C, 34.2; H, 3.9. Found: C, 53.8; H, 4.7. $[Os(PEtPh_2)_3Cl_3]$, $C_{42}H_{45}Cl_3OsP_3$ requires C, 53.7; H, 4.8. Found: C, 47.1; H, 4.3. $[Os(PEtPh_2)_3Br_3]$, $C_{42}H_{45}Br_3OsP_3$ requires C, 47.0; H, 4.2%}.

mer-$[Os(PEt_3)_3Cl_3]$.—An n-butanol (30 cm^3) solution of $Na_2[OsCl_6]$ (0.36 g, 0.8 mmol) was purged with nitrogen, PEt_3 (0.34 g, 2.9 mmol) was added, and the solution refluxed for 2 h. It was cooled, concentrated to *ca.* 5 cm^3, and light petroleum (b.p. 40—60 °C, 5 cm^3) added. After refrigeration for 3 d at 0 °C, the orange crystals produced were filtered off and dried *in vacuo* (0.3 g, 58%) (Found: C, 33.0; H, 7.0. $C_{18}H_{45}Cl_3OsP_3$ requires C, 33.2; H, 6.9%).

The complex *mer*-$[Os(PEt_3)_3Br_3]$ was made similarly (65%) from $Na_2[OsBr_6]$ (Found: C, 27.7; H, 5.9. $C_{18}H_{45}Br_3OsP_3$ requires C, 27.5; H, 5.7%) and similar preparations were used for $[Os(AsEt_3)_3Cl_3]$ (Found: C, 27.5; H, 5.9. $C_{18}H_{45}As_3Cl_3Os$ requires C, 27.6; H, 5.7%) and $[Os(AsEt_3)_3Br_3]$ (Found: C, 23.7; H, 5.1. $C_{18}H_{45}As_3Br_3Os$ requires C, 23.6; H, 4.9%).

mer-$[Os(SbPh_3)_3X_3]$.—A warm nitrogen-purged solution of $SbPh_3$ (1.7 g, 4.8 mmol) in Bu^tOH (15 cm^3) was added to a degassed solution of OsO_4 (0.3 g, 1.2 mmol) and concentrated HX (2 cm^3) in Bu^tOH (20 cm^3). The mixture was refluxed for 2 h then cooled, when the complexes separated out. The solid was washed with ethanol (10 cm^3) and dried *in vacuo* (*ca.* 50%) {Found: C, 47.7; H, 3.3. $[Os(SbPh_3)_3Cl_3]$, $C_{54}H_{45}Cl_3OsSb_3$ requires C, 47.8; H, 3.3. Found: C, 43.5; H, 3.0. $[Os(SbPh_3)_3Br_3]$, $C_{54}H_{45}Br_3OsSb_3$ requires C, 43.5; H, 3.0%}.

fac-$[Os(py)_3X_3]$.—These complexes were prepared from $Na_2[OsX_6]$ and pyridine in dimethylformamide as described by Buckingham *et al.*[24] (Found: C, 33.4; H, 2.9; N, 7.6. $[Os(py)_3Cl_3]$, $C_{15}H_{15}Cl_3N_3Os$ requires C, 33.7; H, 2.8; N, 7.9%).

fac-$[OsL_3Cl_3]$ (L = PMe_2Ph, PEt_2Ph, *or* $AsMe_2Ph$).—These complexes were prepared from the corresponding *mer* isomers *via* the tetrahydrides according to the method of Douglas and Shaw.[12] The tetrahydrides were generated *in situ*, treated with gaseous HCl, and the products purified by recrystallisation from CH_2Cl_2 (*ca.* 35%) {Found: C, 40.6; H, 4.5. $[Os(PMe_2Ph)_3Cl_3]$, $C_{24}H_{33}Cl_3OsP_3$ requires C, 40.5; H, 4.6. Found: C, 34.2; H, 4.0. $[Os(AsMe_2Ph)_3Cl_3]$, $C_{24}H_{33}As_3Cl_3Os$

requires C, 34.2; H, 3.9. Found: C, 45.0; H, 5.6. [Os($PEt_2Ph)_3Cl_3$], $C_{30}H_{45}Cl_3OsP_3$ requires C, 45.3; H, 5.7%}.

[OsL_3X_3]BF_4: *General Method*.—The complex [OsL_3X_3] (*ca.* 0.3 g) was suspended in 40% aqueous HBF_4 (5 cm^3) and cooled in an ice-bath. Concentrated HNO_3 (*ca.* 1 cm^3) was added dropwise, and the reaction mixture stirred at 0 °C. Small portions were withdrawn and checked by u.v.–visible spectra for the disappearance of the characteristic features of the osmium(III) materials. When oxidation was judged complete, the solid product was filtered off, rinsed with water (5 cm^3), and dried *in vacuo* (*ca.* 40%) {Found: C, 17.5; H, 4.4. [Os($PMe_3)_3Cl_3$]BF_4, $C_9H_{27}BCl_3F_4OsP_3$ requires C, 17.7; H, 4.4. Found: C, 14.5; H, 3.7. [Os($PMe_3)_3Br_3$]BF_4, $C_9H_{27}BBr_3F_4OsP_3$ requires C, 14.5; H, 3.6. Found: C, 29.1; H, 6.2. [Os($PEt_3)_3Cl_3$]BF_4, $C_{18}H_{45}BCl_3F_4OsP_3$ requires C, 29.3; H, 6.1. Found: C, 25.0; H, 5.1. [Os($PEt_3)_3Br_3$]BF_4, $C_{18}H_{45}BBr_3F_4OsP_3$ requires C, 24.8; H, 5.2. Found: C, 40.4; H, 5.4. [Os($PEt_2Ph)_3Cl_3$]BF_4, $C_{30}H_{45}BCl_3F_4OsP_3$ requires C, 40.8; H, 5.1. Found: C, 35.7; H, 4.3. [Os($PEt_2Ph)_3Br_3$]BF_4, $C_{30}H_{45}BBr_3F_4OsP_3$ requires C, 35.5; H, 4.4. Found: C, 49.4; H, 4.5. [Os($PEtPh_2)_3Cl_3$]BF_4, $C_{42}H_{45}BCl_3F_4OsP_3$ requires C, 49.1; H, 4.4. Found: C, 43.3; H, 3.8. [Os($PEtPh_2)_3Br_3$]BF_4, $C_{42}H_{45}BBr_3F_4OsP_3$ requires C, 43.5; H, 3.9. Found: C, 25.0; H, 5.1. [Os($AsEt_3)_3Cl_3$]BF_4, $C_{18}H_{45}As_3BCl_3F_4Os$ requires C, 24.8; H, 5.2. Found: C, 21.6; H, 4.6. [Os($AsEt_3)_3Br_3$]BF_4, $C_{18}H_{45}As_3BBr_3F_4Os$ requires C, 21.5; H, 4.5. Found: C, 13.3; H, 2.6. [Os{$S(CH_2CH_2CH_2SMe)_2$}Br_3]BF_4, $C_8H_{18}BBr_3F_4OsS_3$ requires C, 13.2; H, 2.5. Found: C, 28.7; H, 2.3; N, 6.9. *fac*-[Os(py)$_3Cl_3$]BF_4, $C_{15}H_{15}BCl_3F_4N_3Os$ requires C, 29.0; H, 2.4; N, 6.8. Found: C, 23.7; H, 2.2; N, 5.6. *fac*-[Os(py)$_3Br_3$]BF_4, $C_{15}H_{15}BBr_3F_4N_3Os$ requires C, 23.9; H, 2.0; N, 5.6%}.

mer-[Os(py)$_3Cl_3$]Cl. The complex *mer*-[Os(py)$_3I_3$][18] (0.35 g, 0.43 mmol) was dissolved in CH_2Cl_2 (10 cm^3) and a saturated solution of chlorine in CCl_4 was added slowly until the colour changed from dark red to orange. The u.v.–visible spectrum of the solution was monitored to check complete loss of the iodide. The solution was evaporated to dryness and the minimum quantity of CH_2Cl_2 added to dissolve the product, which was reprecipitated by slow addition of toluene. The orange solid was filtered off and dried *in vacuo* (60%) (Found: C, 31.8; H, 2.5; N, 7.4. $C_{15}H_{15}Cl_4N_3Os$ requires C, 31.6; H, 2.6; N, 7.4%).

The complex *mer*-[Os(py)$_3Br_3$]BF_4 was prepared similarly from the iodo-complex and bromine. The initial product was suspended in HBF_4 (2 cm^3) and concentrated HNO_3 (0.5 cm^3) added dropwise. An oily product separated, which was rinsed with water and then extracted into CH_2Cl_2 (10 cm^3). The solution was concentrated *in vacuo* to isolate the solid {30% on [Os(py)$_3I_3$]} (Found: C, 24.1; H, 2.2; N, 5.5. $C_{15}H_{15}BBr_3F_4N_3Os$ requires C, 23.9; H, 2.0; N, 5.6%).

Crystal Structure Determination.—Red air-stable needle crystals [Os($PEt_2Ph)_3Cl_3$]$\cdot CH_2Cl_2$ were isolated from CH_2Cl_2–hexane, mounted in thin-walled glass capillaries, and examined photographically by *X*-ray diffraction. The crystals were very prone to twinning. Diffracted intensities (5 050) were recorded using an Enraf-Nonius CAD4 diffractometer fitted with Mo radiation and a graphite monochromator from a crystal 0.5 × 0.1 × 0.03 mm at ambient temperature (ω—2θ scans; $1.5 < \theta < 23°$; h −20 to 20, k −11 to 11, l 0 to 11). The three intensity controls showed no decay during the experiment and after the data reduction there remained 4 858 unique reflections ($R_{int.}$ = 0.008) of which 3 817 with $F > 2\sigma(F)$ were used in the analysis and refinement. An empirical ψ-scan absorption correction was applied (transmission: minimum, 73.5; maximum, 99.8%). The density was measured by flotation in CCl_4–$C_2H_4Br_2$ mixtures.

Crystal data. $C_{30}H_{45}Cl_3OsP_3\cdot CH_2Cl_2$, M = 880.10, triclinic, space group $P\bar{1}$ (no. 2), a = 18.606(2), b = 10.088(2), c = 10.011(4) Å, α = 107.91(3), β = 97.23(3), γ = 94.85(1)°, U = 1 758.6 Å^3, D_m = 1.65(2) g cm^{-3}, Z = 2, D_c = 1.661 g cm^{-3}, $F(000)$ = 878, Mo-K_α radiation (λ = 0.710 69 Å), μ(Mo-K_α) = 41.1 cm^{-1}.

The structure was solved using the Patterson method and subsequent structure-factor and electron-density syntheses located the remaining non-H atoms. Initially the space group $P1$ was employed, but it appeared that the two independent molecules were related by a centre of symmetry and subsequent analysis was carried out in the centrosymmetric space group $P\bar{1}$. At the later stages of refinement the solvate molecule became clear and a number of phenyl H atoms were indicated in the difference electron-density syntheses. Hydrogen atoms of the phosphine ligand were introduced into the molecule in calculated positions [d(CH) = 0.95 Å] with methyl H atoms being given a common thermal parameter and similarly for methylene and phenyl group H atoms. Full-matrix least-squares refinement minimising $\Sigma w\Delta^2$ converged to R = 0.048 {3 817 reflections, 257 parameters, anisotropic [Os,Cl,P,C(ethyl only)] and isotropic [Cl(CH_2Cl_2),C,H] atoms, $w^{-1} = [\sigma^2(F) + 0.0005F^2]$, maximum shift/error = 0.03, S = 1.30, R' = 0.048}. The residual electron density was in the range 1.09 to −1.03 e Å^{-3}. Atomic scattering factors for neutral atoms and anomalous dispersion corrections were taken from SHELX 76[33] (Cl,P,C,H) and ref. 34 (Os), and all calculations were carried out using the programs SHELX 76[33] and ORTEP II[35] on an IBM3090 computer. Table 6 gives the atomic co-ordinates.

Additional material available from the Cambridge Crystallographic Data Centre comprises H-atom co-ordinates, thermal parameters, and complete bond lengths and angles.

Acknowledgements

We thank the S.E.R.C. for support of this work, Dow Chemicals (TX Division) for leave of absence (to R. A. C.), Professor M. B. Hursthouse for *X*-ray data collection using the S.E.R.C./Q.M.C. service, and N. R. Champness for assistance with the electrochemical measurements.

References

1 Part 34, J. L. Brown, T. Kemmitt, and W. Levason, *J. Chem. Soc., Dalton Trans.*, 1990, 1513.
2 R. A. Cipriano, W. Levason, D. Pletcher, N. A. Powell, and M. Webster, *J. Chem. Soc., Dalton Trans.*, 1987, 1901.
3 R. A. Cipriano, L. R. Hanton, W. Levason, D. Pletcher, N. A. Powell, and M. Webster, *J. Chem. Soc., Dalton Trans.*, 1988, 2483.
4 R. A. Cipriano, W. Levason, R. A. S. Mould, D. Pletcher, and N. A. Powell, *J. Chem. Soc., Dalton Trans.*, 1988, 2677.
5 W. P. Griffith, in 'Comprehensive Coordination Chemistry,' eds. G. Wilkinson, J. A. McCleverty, and R. D. Gillard, Pergamon, Oxford, 1987, vol. 4, p. 635.
6 R. A. Cipriano, W. Levason, R. A. S. Mould, D. Pletcher, and M. Webster, *J. Chem. Soc., Dalton Trans.*, 1990, 339.
7 J. E. Armstrong and R. A. Walton, *Inorg. Chem.*, 1983, **22**, 1545.
8 V. T. Coombe, G. A. Heath, T. A. Stephenson, J. D. Whitelock, and L. J. Yellowlees, *J. Chem. Soc., Dalton Trans.*, 1985, 947.
9 P. E. Fanwick, I. F. Fraser, S. M. Tetrick, and R. A. Walton, *Inorg. Chem.*, 1987, **26**, 3786.
10 J. D. Buhr, J. R. Winckler, and H. Taube, *Inorg. Chem.*, 1980, **19**, 2416.
11 J. Chatt, G. J. Leigh, D. M. P. Mingos, and R. J. Paske, *J. Chem. Soc. A*, 1968, 2636.
12 P. G. Douglas and B. L. Shaw, *J. Chem. Soc. A*, 1970, 334.
13 A. Araneo and C. Bianchi, *Gazz. Chim. Ital.*, 1967, **97**, 885.
14 S. K. Harbron and W. Levason, *J. Chem. Soc., Dalton Trans.*, 1987, 633.
15 J. Chatt, G. J. Leigh, and D. M. P. Mingos, *J. Chem. Soc. A*, 1969, 1674.

16 L. Aslanov, R. Mason, A. G. Wheeler, and P. O. Whimp, *Chem. Commun.*, 1970, 30.
17 C. C. Hinkley, M. Matusz, and P. D. Robinson, *Acta Crystallogr., Sect. C*, 1988, **44**, 1829.
18 A. Scheffler and W. Preetz, *Z. Naturforsch., Teil B*, 1976, **31**, 1099.
19 A. J. Blake, G. A. Heath, G. Smith, L. J. Yellowlees, and D. W. A. Sharp, *Acta Crystallogr., Sect. C*, 1988, **44**, 1836.
20 R. Ali, S. J. Higgins, and W. Levason, *Inorg. Chim. Acta*, 1984, **84**, 65.
21 E. G. Hope, W. Levason, S. G. Murray, and G. L. Marshall, *J. Chem. Soc., Dalton Trans.*, 1985, 2185.
22 B. Bell, J. Chatt, and G. J. Leigh, *J. Chem. Soc., Dalton Trans.*, 1973, 997.
23 P. R. Brookes, C. Masters, and B. L. Shaw, *J. Chem. Soc. A*, 1971, 3756.
24 D. A. Buckingham, F. P. Dwyer, H. A. Goodwin, and A. M. Sargeson, *Aust. J. Chem.*, 1964, **17**, 315.
25 J. Lewis, F. E. Mabbs, and R. A. Walton, *J. Chem. Soc. A*, 1967, 1366.
26 Cambridge Structural Database, Cambridge Crystallographic Data Centre, University of Cambridge.
27 E. W. Randall and D. Shaw, *J. Chem. Soc. A*, 1969, 2867.
28 F. A. Cotton and R. L. Luck, *Inorg. Chem.*, 1989, **28**, 2181.
29 G. J. Leigh and D. M. P. Mingos, *J. Chem. Soc. A*, 1970, 587.
30 A. J. McCaffery and M. D. Rowe, *J. Chem. Soc., Faraday Trans. 2*, 1973, 1767.
31 A. J. McCaffery and M. D. Rowe, *J. Chem. Soc., Faraday Trans. 2*, 1973, 1779.
32 A. B. P. Lever, 'Inorganic Electronic Spectroscopy,' 2nd edn., Elsevier, Amsterdam, 1984.
33 G. M. Sheldrick, SHELX 76, Program for Crystal Structure Determination, University of Cambridge, 1976.
34 'International Tables for *X*-Ray Crystallography,' Kynoch Press, Birmingham, 1974, vol. 4, pp. 99—101.
35 C. K. Johnson, ORTEP II, Report ORNL-5138, Oak Ridge National Laboratory, Tennessee, 1976.

Received 8*th February* 1990; *Paper* 0/00583E